This article was downloaded by:
On: *25 January 2011*
Access details: *Access Details: Free Access*
Publisher *Taylor & Francis*
Informa Ltd Registered in England and Wales Registered Number: 1072954 Registered office: Mortimer House, 37-41 Mortimer Street, London W1T 3JH, UK

Liquid Crystals

Publication details, including instructions for authors and subscription information:
http://www.informaworld.com/smpp/title~content=t713926090

Studies on the electro-optical properties of polymer stabilised cholesteric liquid crystal/aerosil particles composites

Xiaokai Liang[a]; Hui Cao[a]; Guohui Pan[a]; Xiaopeng Cui[a]; Fasheng Li[a]; Guoguang Niu[a]; Duowei Zhang[a]; Zhou Yang[a]; Huai Yang[a]; Siquan Zhu[ab]
[a] Department of Materials Physics and Chemistry, School of Materials Science and Engineering, University of Science and Technology Beijing, Beijing 100083, People's Republic of China [b] Department of Ophthalmology, Tongren Hospital, Capital Medical University, Beijing, People's Republic of China

To cite this Article Liang, Xiaokai , Cao, Hui , Pan, Guohui , Cui, Xiaopeng , Li, Fasheng , Niu, Guoguang , Zhang, Duowei , Yang, Zhou , Yang, Huai and Zhu, Siquan(2009) 'Studies on the electro-optical properties of polymer stabilised cholesteric liquid crystal/aerosil particles composites', Liquid Crystals, 36: 1, 93 — 100

To link to this Article: DOI: 10.1080/02678290802680805

URL: http://dx.doi.org/10.1080/02678290802680805

PLEASE SCROLL DOWN FOR ARTICLE

Full terms and conditions of use: http://www.informaworld.com/terms-and-conditions-of-access.pdf

This article may be used for research, teaching and private study purposes. Any substantial or systematic reproduction, re-distribution, re-selling, loan or sub-licensing, systematic supply or distribution in any form to anyone is expressly forbidden.

The publisher does not give any warranty express or implied or make any representation that the contents will be complete or accurate or up to date. The accuracy of any instructions, formulae and drug doses should be independently verified with primary sources. The publisher shall not be liable for any loss, actions, claims, proceedings, demand or costs or damages whatsoever or howsoever caused arising directly or indirectly in connection with or arising out of the use of this material.

Liquid Crystals,
Vol. 36, No. 1, January 2009, 93–100

Studies on the electro-optical properties of polymer stabilised cholesteric liquid crystal/aerosil particles composites

Xiaokai Liang[a], Hui Cao[a], Guohui Pan[a], Xiaopeng Cui[a], Fasheng Li[a], Guoguang Niu[a], Duowei Zhang[a], Zhou Yang[a], Huai Yang[a]* and Siquan Zhu[ab]*

[a]*Department of Materials Physics and Chemistry, School of Materials Science and Engineering, University of Science and Technology Beijing, Beijing 100083, People's Republic of China;* [b]*Department of Ophthalmology, Tongren Hospital, Capital Medical University, Beijing, People's Republic of China*

(Received 19 September 2008; final form 10 December 2008)

Normal-mode polymer stabilised cholesteric liquid crystal (Ch-LC)/aerosil particles (APs) composites are prepared by photo-polymerisation of the photo-polymerisable monomer in the electrically induced homeotropically oriented cholesteric phase of a photo-polymerisable monomer/Ch-LC/APs mixture. On the application of an electric field, the composites can change from a light scattering state to a transparent state accompanied by the texture changing from a focal conic texture to an electrically induced homeotropic texture. Moreover, the process was greatly influenced by the addition of the APs. The focus of this study is on the effects of the APs on the electro-optical performance and the morphology of polymer network of the composites. The effect of the chiral dopant concentration on the electro-optical performance is also studied.

Keywords: electro-optical performance; aerosil particles; morphology; liquid crystals

1. Introduction

Recently, polymer stabilised liquid crystals (PSLCs) have received great interest for their use in display devices and optical telecommunications, as well as for the fundamental insights that they provide on liquid crystal (LC)/polymer composites (*1–5*). The normal-mode polymer stabilised cholesteric texture (PSCT) is one example of these systems, in which a low concentration of photo-polymerisable monomer is dissolved in the cholesteric liquid crystal (Ch-LC). Then the mixture is injected into an empty cell without any surface treatment. A normal-mode cell is irradiated by ultraviolet (UV) light in the homeotropic texture in the presence of an electric field. When the field is removed after the photo-polymerisation, the LC in the vicinity of the polymer tends to remain perpendicular to the cell surfaces while the remaining LCs relax back to the spiral structure. A focal conic texture is formed as the result of the competition between the intrinsic spiral structure and the constraining effect of the polymer. In this case, incident light is strongly scattered, and the cell is opaque. When an electric field is applied, the LC is transformed into the homeotropic texture and the cell becomes clear. The process of applying voltage is in fact the change from the focal conic to the homeotropic texture in which the helical structure is unwound with the LC director perpendicular to the cell surface (*6*). The whole process is shown in Figure 1.

Nematic LC/aerosil particles (APs) composites have been studied extensively (*1, 7–9*), but to the best of the authors' knowledge, the effect of APs on PSCT has been less reported although the addition of APs must provide some changes to the electro-optical properties of PSCT. Therefore, in this study, polymer stabilised Ch-LC/APs composites are prepared and the effects of the APs on the electro-optical properties of the composites are investigated.

2. Experiments

2.1 *Materials*

The Ch-LC used was a mixture of nematic LC SLC-1717 (Slichem Liquid Crystal Material Co, Ltd) and chiral dopant CB15 (Merck Co, Ltd). The pitch length, *p*, of the Ch-LC was controlled by the content of CB15, *C*, according to the equation $HTP=1/PC$, where the helical twisting power (HTP) of CB15 is a constant at 298.0 K. The photo-polymerisable LC diacrylate monomer, MBAHB, which is synthesised according to the method suggested by Broer (*10*), was dissolved in the Ch-LC. MBAHB used in this experiment has a structure including a mesogenic core, reactive end groups, and flexible alkyl spacer chains between the core and the end groups (*11, 12*). A small amount of the photo-initiator, 2,2-dimethopxy-1,2-diphenyl-ethanone (IRG651, TCI Co, Ltd), was added to the mixture to initiate

---

*Corresponding author. Email: yanghuai@mater.ustb.edu.cn / siquanzhu@sina.com

ISSN 0267-8292 print/ISSN 1366-5855 online

DOI: 10.1080/02678290802680805
http://www.informaworld.com

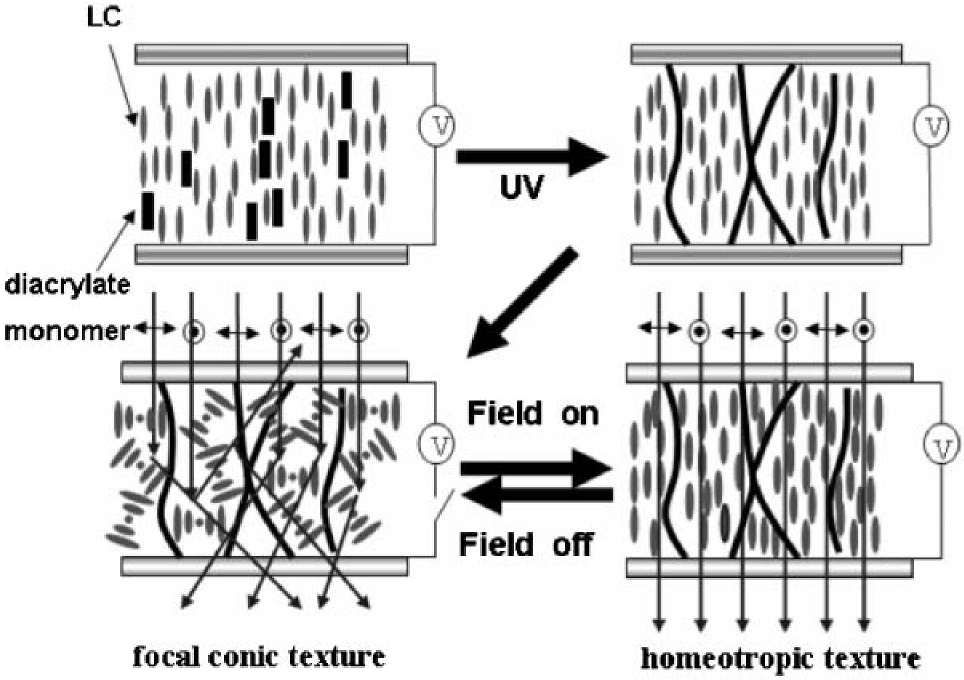

Figure 1. Schematic diagram of normal-mode polymer stabilised cholesteric texture (PSCT).

polymerisation of MBAHB, and the amount added was 5.0 wt% of the monomer. Under UV irradiation, the MBAHB polymerised to produce a cross-linked anisotropic polymer network. Figure 2 shows the chemical structures of the materials used. In this experiment, we had prepared samples A_0, B_0, C_0 and D_0 for a comparison. The weight ratios of MBAHB/SLC1717/CB15 were 3.5/87.8/8.7, 3.5/86.9/9.6, 3.5/85.9/10.6 and 3.5/84.9/11.6 for samples A_0, B_0, C_0 and D_0 which contained no APs, respectively. The pitch lengths of samples A_0, B_0, C_0 and D_0 were 1.4, 1.3, 1.2 and 1.1 μm, respectively. The hydrophobic APs we used in this experiment were Aerosil R812S (Degussa-Hüls Co, Ltd) with a primary size of 7.0 nm. The compositions of the studied samples, A_1–A_6, B_1–B_6, C_1–C_6 and D_1–D_6, are listed in Table 1. To prepare the polymer stabilised Ch-LC/APs composites, the initial mixtures were dissolved in acetone and stirred for about 2.0 hours away from light to achieve good dispersion. Then, the samples were placed in a vacuum system at 10^{-3} Torr for 24 hours to ensure that acetone had been volatilised off.

2.2 *Preparation of samples*

The inner surfaces of the indium-tin oxide (ITO) glass substrates did not need any surface treatment, and 18 μm thick polyethylene terephthalate (PET) films were used as the cell spacers. Subsequently, the empty cell was filled with the mixture by capillary action. To induce photo-polymerisation, the cell that contained the sample was irradiated by UV light (1.80 mW cm^{-2}) for an hour at 298.0 K in the homeotropic texture in the presence of an externally applied electric field. As a result, the crosslinking of MBAHB between the molecules was induced.

2.3 *Measurements*

The electro-optical performances were studied using a LC composition parameter instrument (LCT-5016C, Changchun Liancheng Instrument Co, Ltd). Polarising optical microscopy (POM) (Olympus BX-51) was used to observe the dispersion of APs in the mixture, and the POM micrograph of the texture without any photo-polymerisation is shown in Figure 3. We used the average transmittance over the visible spectrum as the measure of transmittance, and the transmittance of air was normalised as 100%. The polymer network was observed using scanning electron microscopy (SEM) (Cambridge S360). The samples were prepared in the following way. First, the sealant material of the cell was removed to allow the diffusion of hexane into the cell, after UV irradiation of the cell for photo-polymerisation. Second, the cell was dried *in vacuo* for a few hours after the LC was extracted with hexane. Finally, the cell was opened with caution and the substrate plus polymer network were coated with a thin gold layer to eliminate any electric charge problems in the SEM study.

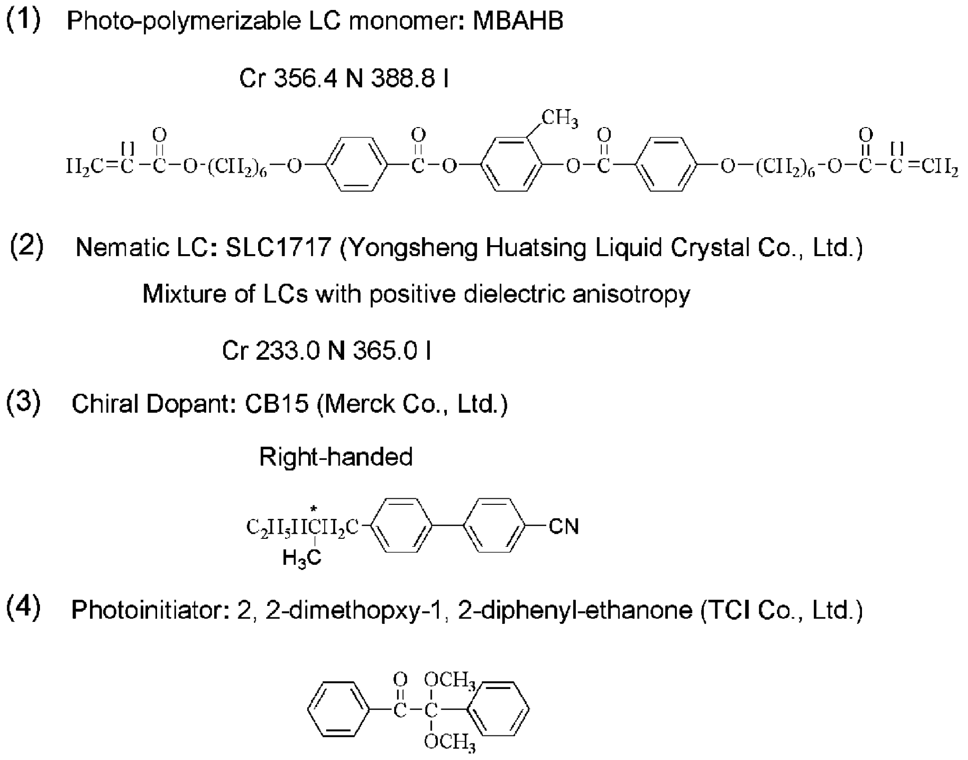

Figure 2. The chemical structures and some physical parameters of the materials used.

3. Results and discussion

3.1 *Electro-optical performance*

Figure 4 shows the electro-optical performance of samples A_1–A_6, with different concentrations of the APs. The electro-optical performance in this paper includes threshold voltage (V_{th}), saturation voltage (V_{sat}), field-on response time (T_{on}), field-off response time (T_{off}) and contrast. The threshold voltage (V_{th}) is defined as the applied voltage when the transmittance reaches 10% of the transmittance of air, and under this voltage, the unwind process has already begun. When the applied voltage reaches V_{sat}, the transmittance is 90% of the transmittance of air, and the unwind process is close to completion. The field-on and field-off response times T_{on} and T_{off} are defined as the time for the transmittance going from 10% to 90% (or 90% to 10%) of the total change between the on and off states. The field-on response time T_{on} indicates the time that the entire unwind process takes, whereas the field-off response time T_{off} is the time that the process of going back to a helical structure takes. The contrast is defined as the ratio of the highest final transmittance to the lowest initial transmittance.

The voltage dependence of the transmittances for samples A_1–A_6 is shown in Figure 4(a). With the increase in the applied voltage, the change from an opaque focal conic texture to a clear homeotropic texture can be easily observed. As the AP concentration increases, V_{th} and V_{sat} both decrease, which can be seen more clearly in Figure 4(b). The reason for this may be that the addition of the APs raises the resistance of the diffusion of the free radicals from the monomer in the process of UV irradiation, leading to the formation of a tighter polymer network. The elastic interaction between the polymer network and LC is getting stronger with the increase in the

Table 1. The ratios (wt%) of the materials of the samples A_1–D_6.

Samples	A_0/R812S (wt%)	Samples	B_0/R812S (wt%)	Samples	C_0/R812S (wt%)	Samples	D_0/R812S (wt%)
A_1	100.0/0.0	B_1	100.0/0.0	C_1	100.0/0.0	D_1	100.0/0.0
A_2	99.9/0.1	B_2	99.9/0.1	C_2	99.9/0.1	D_2	99.9/0.1
A_3	99.7/0.3	B_3	99.7/0.3	C_3	99.7/0.3	D_3	99.7/0.3
A_4	99.5/0.5	B_4	99.5/0.5	C_4	99.5/0.5	D_4	99.5/0.5
A_5	99.2/0.8	B_5	99.2/0.8	C_5	99.2/0.8	D_5	99.2/0.8
A_6	99.0/1.0	B_6	99.0/1.0	C_6	99.0/1.0	D_6	99.0/1.0

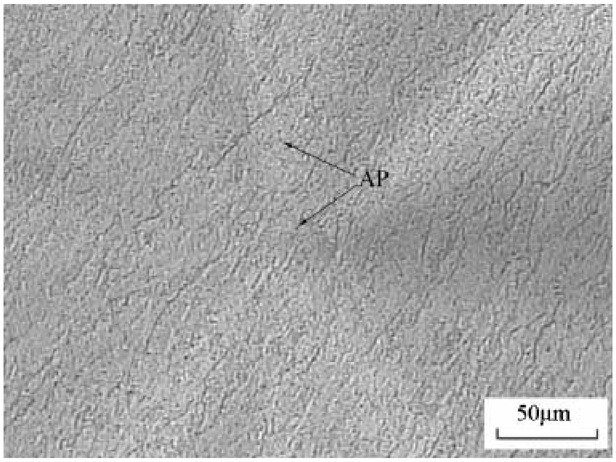

Figure 3. POM micrograph of the texture without any photo-polymerisation.

concentration of the APs, and less energy is needed to complete the unwind process. As shown in Figure 4(b), the decrease in the driving voltage from sample A_1 to A_2 is much more drastic compared with the latter components. Figure 4(c) presents the concentration of the APs dependence on the response time for samples A_1–A_6.nThe field-on response time T_{on} decreases with the increase in concentration of the APs, whereas the curve of T_{off} concentration appears to have the opposite tendency. This is because the stronger elastic interaction between the polymer network and LC, which is caused by the increase in the concentration of the APs, leads to less time for unwinding the helical structure. However, more time is needed for the system to go back to the original helical structure. Figure 4(d) shows the concentration of APs dependence on the contrast, from which it can be seen that with the increase in the concentration of the APs, the contrast decreases. From Figure 5, the tendency of the curve can be seen more clearly. As shown in Figure 5(b), the initial transmittance of the sample rises with the increasing APs content, while the transmittance of the homeotropic state of the sample is barely affected by APs. In the initial focal conic texture state, after the removal of the applied electric field, because of the strong anchoring of the APs, not only the LC molecules in the vicinity of the polymer tend to

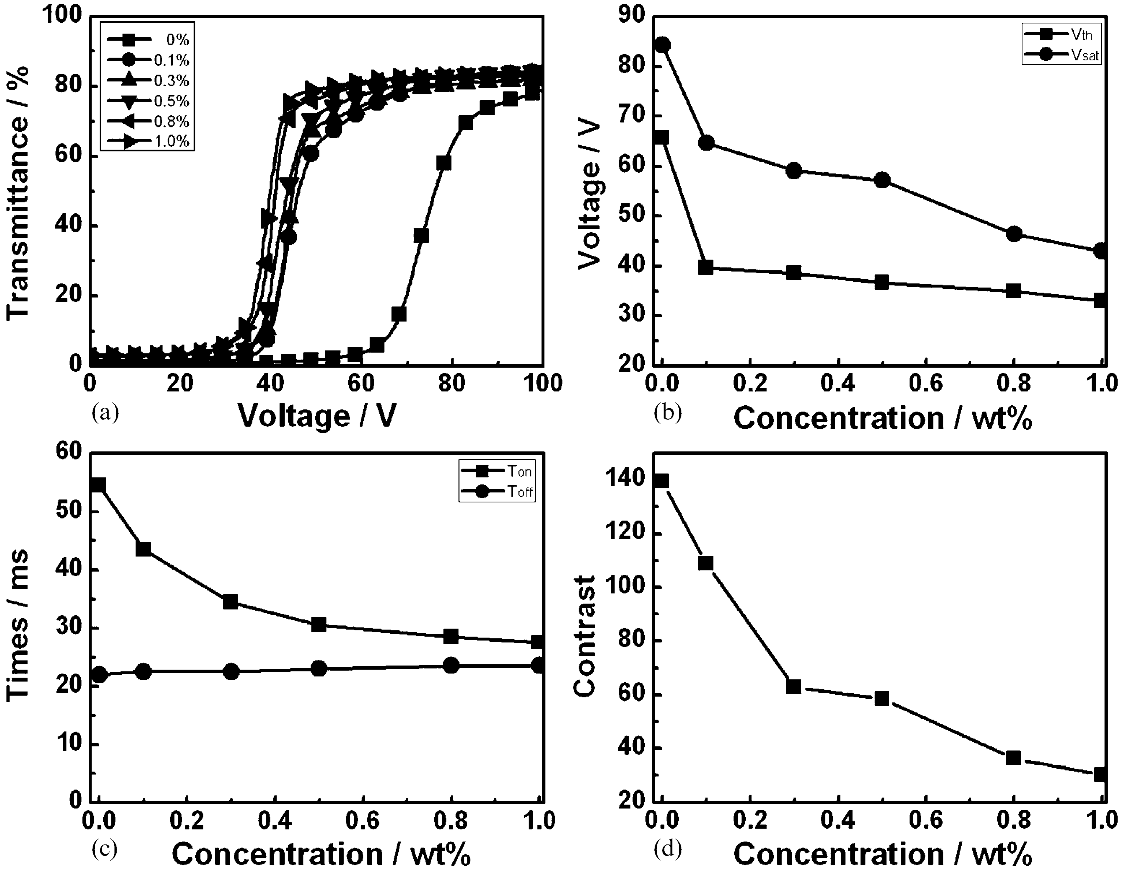

Figure 4. The electro-optical performance of samples A_1–A_6: (a) plot of the voltage dependence on the transmittance; (b) plot of the concentration of APs dependence on V_{th} and V_{sat}; (c) plot of the concentration of the APs dependence on the response times; (d) plot of the concentration of APs dependence on the contrast.

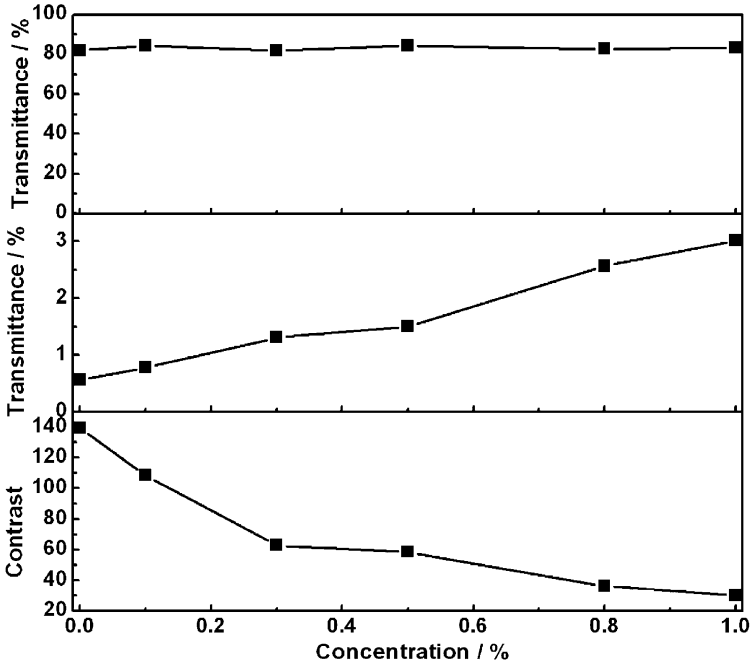

Figure 5. The electro-optical performance of samples A_1–A_6: (a) plot of the concentration of APs dependence on the final transmittance; (b) plot of the concentration of the APs dependence on the initial transmittance; (c) plot of the concentration of APs dependence on the contrast.

remain perpendicular to the surface, but the LC molecules in the local region close to the APs still keep and approximately homeotropic texture, whereas the LC molecules far away from the APs can relax back to the spiral structure. This leads to the decrease of the scattering domains and the increase of the initial transmittance with the increasing APs content. In the homeotropic texture state, where the LC molecule is oriented well and the defects caused by APs have been reduced, the transmittance is affected little (*13*), as shown in Figure 5(a). According to the definition of the contrast, which is the ratio of the final transmittance to the initial transmittance, we can conclude that the contrast decreases with the increase in the concentration of the APs as shown in Figure 5(c), because even a little change of the denominator can significantly influence the ratio.

The characteristics of the electro-optical performance for samples B_1–B_6, C_1–C_6 and D_1–D_6 are similar to that of samples A_1–A_6.

The concentration of the chiral dopant dependence of the electro-optical performance has also been studied. Take the samples of A_3–D_3 as an example, for which the concentrations of the APs are identical, which is 0.3%, and the electro-optical performance of these samples is shown in Figure 6. Figure 6(a) shows the voltage dependence of the transmittances for samples A_3–D_3, and from Figure 6(b), it is demonstrated that the concentration of the chiral dopant has an approximately linear relationship with the threshold voltage as well as with the saturation voltage. This means that with the increase in the chiral dopant concentration, both V_{th} and V_{sat} rise. From the point of view of energy, it is reasonable to believe that more energy is needed to unwind the helical structure with the decrease in the pitch length caused by the increasing concentration of the chiral dopant. The concentration of the chiral dopant dependence of the response time for samples is shown in Figure 6(c), which demonstrates that with the increase in the concentration of the chiral dopant, T_{on} increases and T_{off} decreases. The result can be easily explained from the point of view of energy. Finally, the pitch length is one of the most important factors that determine the light scattering domain size. With the increase in the chiral dopant, the pitch length decreases, causing an increase in the initial light scattering intensity and an increase in the contrast, which is shown in Figure 6(d).

3.2 *The morphology of polymer network*

Figure 7 shows the morphology of fractured surface, and the fibrous polymer network perpendicular to the substrate can be observed. The network is composed of polymer strands oriented along the direction of the director.

Figure 8 shows the morphology of the polymer network of the different concentrations of the APs

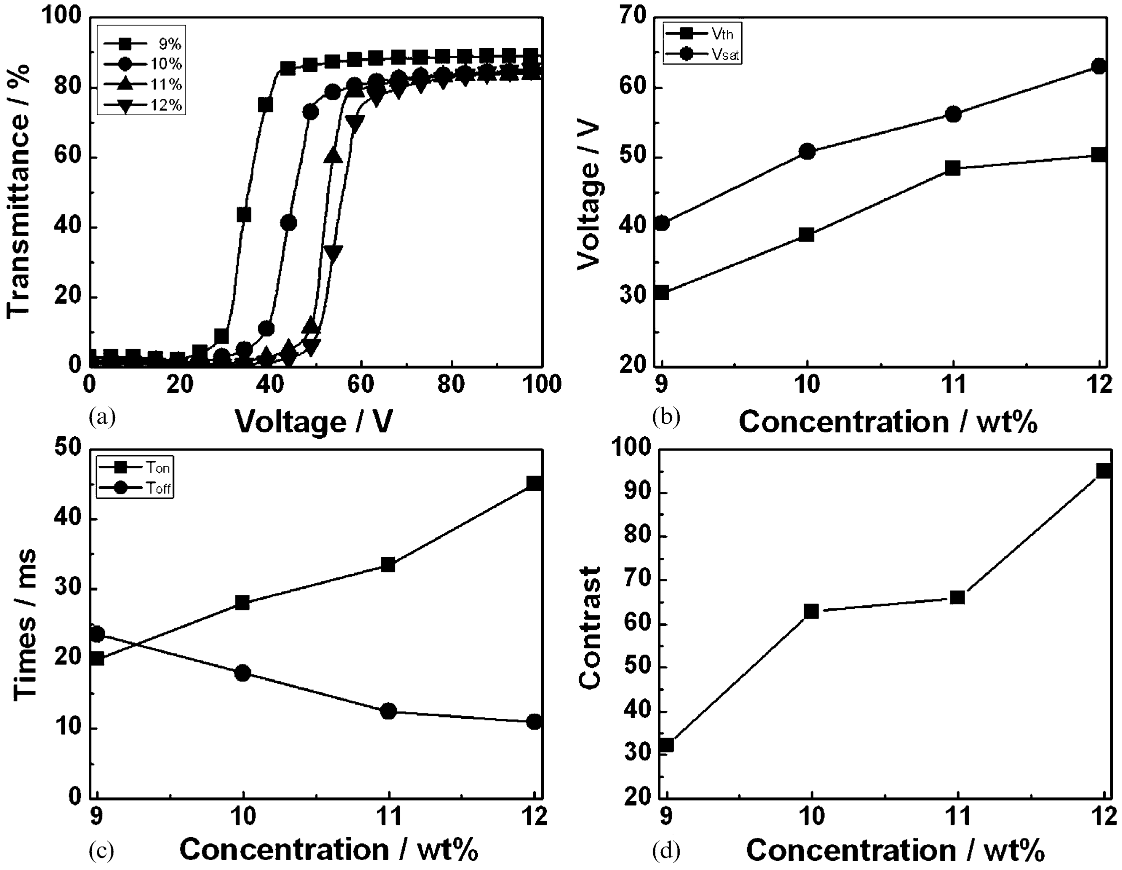

Figure 6. The electro-optical performance of samples A_3–D_3: (a) plot of the voltage dependence on the transmittance; (b) plot of the concentration of monomer dependence on V_{th} and V_{sat}; (c) plot of the concentration of the monomer dependence on the response times; (d) plot of the concentration of the monomer dependence on the contrast.

for samples A_1–A_6. The mesh in the photograph of each sample becomes smaller with the increase in the concentration of the APs. One reason is that as the concentration of the APs increases, the resistance of the diffusion of the free radicals from the monomer becomes greater, and consequently the denser network and smaller mesh are acquired. On the other hand, the APs may serve as the polymerisation centres; therefore, the higher the AP concentration is, the smaller the network ‘grid’ and thinner the network ‘line’ are, and consequently the larger the polymer–LC interfaces area is, and thereby the stronger interaction between the polymer network and the LC is. In particular, compared with sample A_1, a drastic decrease in the mesh size can be observed in sample A_2, which matches the phenomenon of the drastic decrease in the driving voltage between samples A_1 and A_2, as shown in Figure 4. This proves that the addition of APs to the pure PSCT system can obviously change the electro-optical performances of the system, but after that, the change in the electro-optical performance caused by the increase in APs becomes much milder.

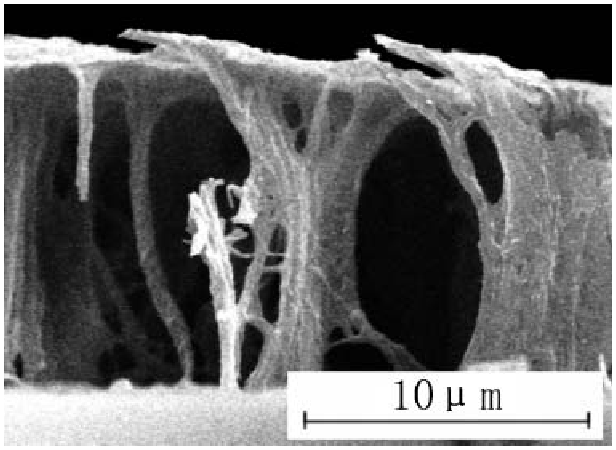

Figure 7. SEM photograph of the homeotropically oriented polymer network from the point of view of a fractured surface.

4. Conclusions

In this paper, the electro-optical performance and the morphology of polymer network of the polymer

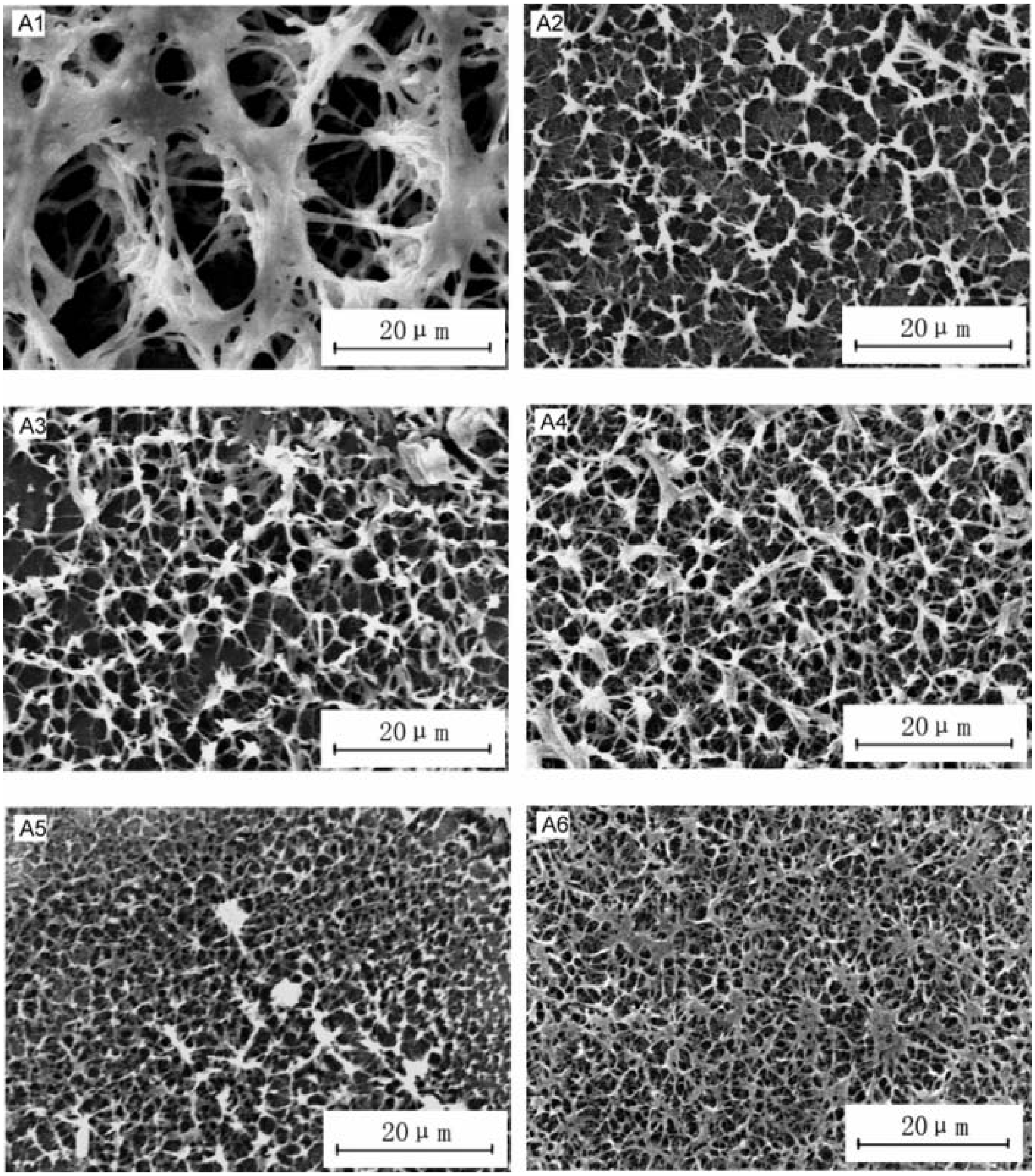

Figure 8. SEM photographs of the homeotropically oriented polymer network of samples A_1–A_6.

stabilised Ch-LC/APs composites have been investigated. In this study we have examined the effect of the APs concentration on the electro-optical performance and the morphology of the polymer network, and the experimental results have revealed that with the increase in the concentration of the APs, the threshold voltage and the saturation voltage both decreased, T_{on} decreased and the T_{off} increased, the initial transmittance increased and the contrast decreased. SEM showed that the increasing APs concentration led to the denser polymer networks with smaller meshes. In addition, the concentration of the chiral dopant dependence on the electro-optical performance has been studied. The results indicate that as the concentration of the chiral dopant increased, both the threshold voltage and the saturation voltage increased, T_{on} increased and T_{off} decreased and the contrast increased.

Acknowledgements

Support from the National Basic Research Program of China (Grant No. 2007CB613301), Projects of the Chinese National Science and Technology Tackling Key Problems (Grant

No. 2006BAI03A09) and the Science and Technology Program of Beijing (Grant No. Y0405004040121) is gratefully acknowledged.

References

(1) Crawford G.P.; Zumer S. *Liquid Crystals in Complex Geometries*; Taylor & Francis: London, 1996; pp. 307–324.
(2) Huang C.Y.; Ke S.W.; Chih Y.S. *Opt. Commun.* **2006**, *266*, 198.
(3) Dierking I.; Kosbar L.L.; Lowe A.C.; Held G.A. *Liq. Cryst.* **1998**, *24*, 387.
(4) Lin Y.L.; Ren H.; Fan Y.H.; Wu Y.H.; Wu S.T. *J. Appl. Phys.* **2005**, *98*, 043112.
(5) Du F.; Lu Y.Q.; Ren H.W.; Gauza S.; Wu S.T. *J. Appl. Phys.* **2004**, *43*, 7083.
(6) Yang D.K.; Chien L.C.; Doane J.W. *Appl. Phys. Lett.* **1992**, *60*, 3102.
(7) Kreuzer M.; Tschudi T.; Eidenschink R. *Appl. Phys. Lett.* **1993**, *62*, 1712.
(8) Dolgov L.O.; Yaroshchuk O.V. *Colloid Polym. Sci.* **2004**, *282*, 1403.
(9) Sikharulidze D. *Appl. Phys. Lett.* **2005**, *86*, 033507.
(10) Broer D.J.; Boven J.; Mol G.N. *Makromol. Chem.* **1989**, *190*, 2255.
(11) Geibel K.; Mammerschmidt A.; Stroher F. *Adv. Mater.* **1995**, *5*, 107.
(12) Broer D.J.; Lub J.; Mol G.N. *Nature* **1995**, *378*, 467.
(13) Li B.F.; Huang H.; Yang H. *Liq. Cryst.* **2008**, *35*, 49.